PRAMANA
—journal of
physics

Vol. 53, No. 1,
July 1999
pp. 93–106

Phase transitions in Langmuir monolayers

K A SURESH* and A BHATTACHARYYA
Raman Research Institute, Bangalore 560 080, India
* E-mail suresh@rri.ernet.in

Abstract. Some fatty acids, lipids, polymers and mesogenic molecules which are amphiphilic in nature spread at the air-water interface to form stable Langmuir monolayers. They exhibit a rich variety of two-dimensional (2D) phases. In this article, we briefly review some of the novel features we have found in these monolayers. For example, we find transition from a 2D monolayer to three-dimensional structures possessing liquid crystalline order, induced liquid condensed phase, demixing of liquid expanded phase, critical points and pattern formation.

Keywords. Langmuir monolayers; liquid crystals; phase transitions; critical phenomena.

PACS Nos 68.15+e; 61.30-v; 05.70.Fh

1. Introduction

An amphiphilic molecule has a hydrophilic head-group at one end and a hydrophobic chain at the other end. Such molecules spread spontaneously at an air–water interface to form monomolecular films called Langmuir monolayers [1]. These monolayers are two-dimensional (2D) systems exhibiting a variety of 2D phases. A typical phase sequence seen on increasing the surface molecular density is gas (G), liquid expanded (LE), liquid condensed (LC), solid and collapsed state.

In analogy with bulk pressure, here one studies the surface pressure π, which is defined as

$$\pi = \gamma_0 - \gamma, \tag{1}$$

where γ_0 is the surface tension of pure water, and γ that of water with the monolayer.

The monolayer is formed on a liquid subphase which is usually high purity water (Millipore Milli-Q) contained in a teflon trough. The monolayer is compressed using a teflon barrier to vary the surface molecular density or surface pressure. Surface pressure is measured by determining the force acting on a plate (platinum blade or filter paper) [1], which is in contact with the subphase. The plate is suspended from a force transducer which measures the force acting on it. The measurement of π as a function of area per molecule (A_m) is called surface manometry.

To study the monolayer phases, techniques like surface manometry and epifluorescence [2] microscopy are widely used. In epifluorescence microscopy, the monolayer is doped with a dye at a molar concentration of about 1%. Then the monolayer is observed under the fluorescence microscope. The different monolayer phases are identified by the different fluorescent intensity levels. For example, the G phase appears dark under the

microscope due to the low density of molecules in this phase and quenching of the dye by the subphase namely water. On the other hand, the LE phase has a higher density and it appears bright. In the LC phase, the molecular arrangement is very compact, hence the dye molecules are expelled. This makes the LC phase also to appear dark. In the case of some three-dimensional (3D) structures like multilayer domains, the intensity of a domain is a measure of its thickness. Further probing of the thick multilayer domains can be undertaken with reflection and polarising microscopy. Reflection studies provide information on the surface topography of the domains. Polarising microscopy is used to identify the molecular ordering of the thicker domains.

It may be remarked here that in recent times, detailed phase identifications [3–5] of monolayer phases have also been carried out based on miscibility and x-ray diffraction studies. In these studies, the LE phase is called L_1. The LC phase is generally called L_2 and is further classified depending on minute structural differences into L_{2d}, L_{2h} etc.

2. Transition from a 2D monolayer to 3D structures

Some amphiphilic compounds can exhibit thermotropic liquid crystalline phases in bulk. As is to be expected, they also form stable 2D Langmuir monolayers [6, 7]. Interestingly, in some cases, these 2D monolayers transform to 3D multilayers [8–10]. We describe here the interesting structures seen in 4′-*n*-octyl-4-cyanobiphenyl (8CB) monolayer [11]. At room temperature, the multilayer domains have thicknesses of the order of a fraction of a micrometre (μm) and exhibit a smectic A phase. On increasing the temperature, these multilayer domains undergo a phase transition resulting in very thick (1 to 40 μm) lens-like domains. In the temperature range 28°C to 36°C, these domains exhibit a nematic phase and above 36°C they exhibit an isotropic phase.

The $\pi - A_m$ isotherms at different temperatures are shown in figure 1. The plateau at A_m greater than 60 Å^2 represents the G and LE two phase region. The region with steeply increasing π ($A_m \sim 48$–55 Å^2) is the LE phase. The region below $A_m \sim 48$ Å^2 corresponds to the co-existence of LE and 3D domains.

The phases indicated by $\pi - A_m$ studies were investigated by epifluorescence microscopy with the dye 4-(hexadecylamino)-7-nitrobenz-2 oxa-1,3 diazole (NBD-HDA). In the G–LE two phase co-existence region, the G phase appeared dark and the LE phase appeared bright. On compression, the whole monolayer became uniformly bright ($A_m \sim 55$ Å^2), indicating the onset of LE phase. At 25°C, circular domains (D_1) brighter than the background LE phase appeared on compressing to $A_m \approx 48$ Å^2. These D_1 domains correspond to a three layer structure. The 3 layer structure is formed at this A_m since the 8CB molecules expelled from the monolayer form an interdigited bilayer above the monolayer. This is consistent with the bilayer formation in 8CB in the bulk. At still lower A_m, similar formation of bilayers above the 3 layer structures can lead to $5, 7, 9, \ldots$ layered structures. Accordingly, on further compression, even before the D_1 domains occupied the entire surface, new and still brighter domains (D_2) appeared around $A_m \approx 20$ Å^2. The D_2 domains exhibit different intensity levels (figure 2a, b) indicating different thicknesses. Here the D_2 and D_1 domains co-existed with the LE phase. The thicknesses of the D_2 domains was found to be of the order of a fraction of a μm. On heating the monolayer, the nature of the domains underwent a transformation. Between

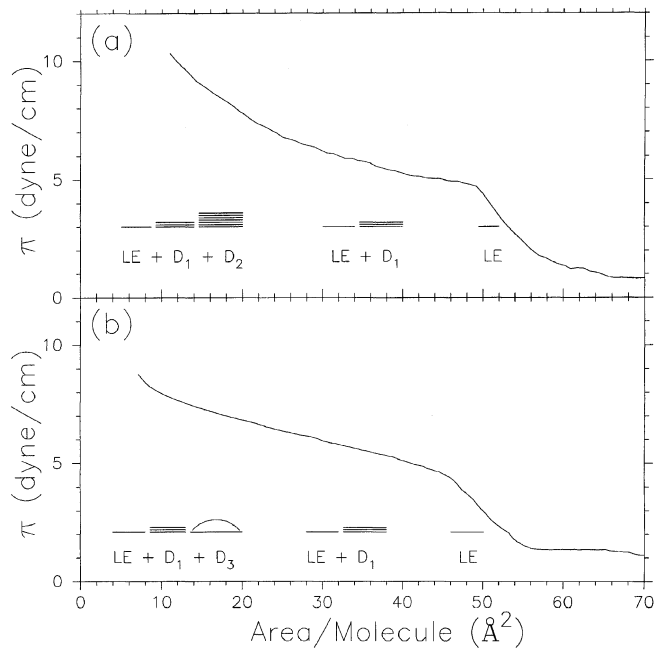

Figure 1. Surface pressure (π)-area per molecule isotherms at two temperatures for 8CB monolayer. The different structures observed are shown schematically. Here D_1 represents the three layer phase, D_2 the optically flat domains and D_3 the lens shaped domains. (**a**) 25°C, (**b**) 35°C.

28°C and 36°C, on compression, D_1 domains appeared in the LE phase around $A_m \approx 45$ Å^2 and co-existed with the LE phase. Further, around $A_m \approx 20$ Å^2, instead of the large D_2 domains, smaller domains (D_3) of much higher brightness and thickness appeared. The D_3 domains were much thicker and of different thicknesses as they were seen in focus at different focal planes (figure 2c). The thicknesses were in the range 1–40 μm. Above 36°C, on compression, D_3 domains appeared in the LE phase around $A_m \approx 45$ Å^2. Interestingly, on expansion, the domains revert slowly to the LE phase.

The surface topography of D_2 and D_3 domains can be obtained using reflection microscopy. In reflection, the LE phase and the D_1 domains were not visible as they were very thin. When the monolayer was compressed below $A_m \approx 20$ Å^2, either D_2 or D_3 domains were seen depending on temperature. Below 28°C, the D_2 domains exhibited different but uniform colours (figure 3a). The colours were due to the interference between light reflected from the air–domain interface and the domain–water interface. The uniformity of colour in a domain indicated its optical flatness. Above 28°C, the D_2 domains changed to D_3 and developed interference rings (figure 3b, c). The ring structure indicated varying thickness. On heating, each such domain decreased in size (area) while the number of rings increased. This indicated growth of the domain in the third dimension. These features were seen even up to 40°C. On cooling, around 28°C, the rings slowly disappeared giving rise to a uniformly coloured region of much larger area. This indicates a reverse transition from D_3 to D_2 domains.

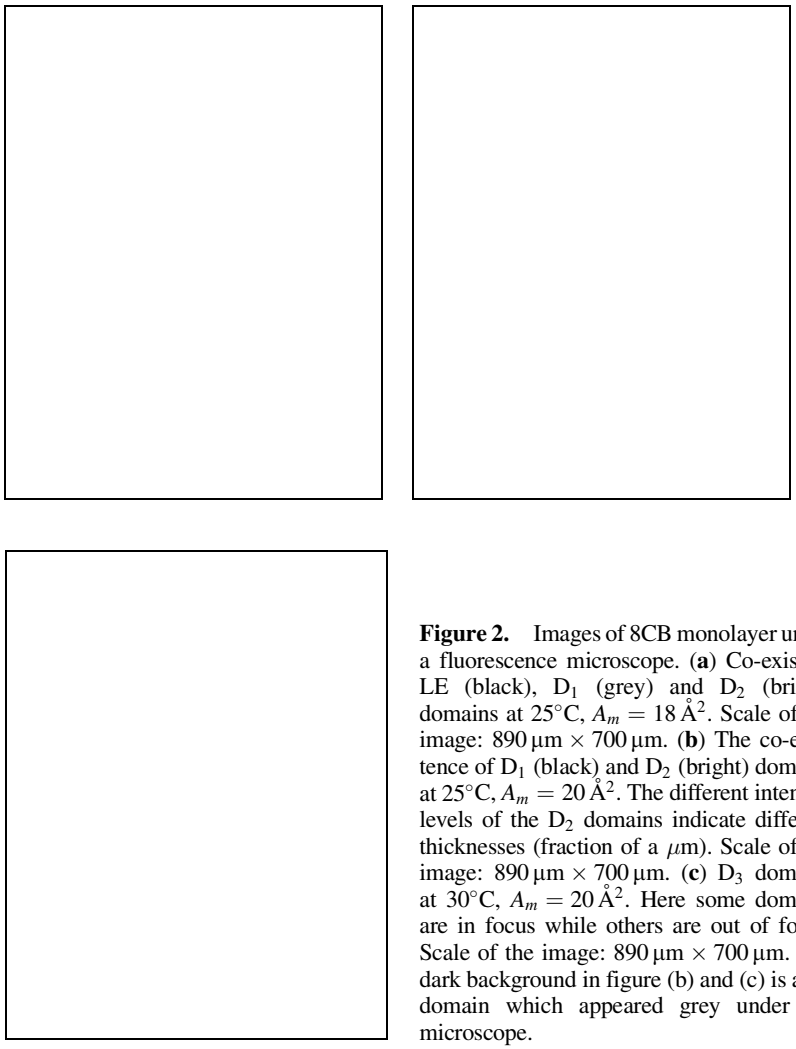

Figure 2. Images of 8CB monolayer under a fluorescence microscope. (**a**) Co-existing LE (black), D_1 (grey) and D_2 (bright) domains at 25°C, $A_m = 18\,\text{Å}^2$. Scale of the image: 890 μm × 700 μm. (**b**) The co-existence of D_1 (black) and D_2 (bright) domains at 25°C, $A_m = 20\,\text{Å}^2$. The different intensity levels of the D_2 domains indicate different thicknesses (fraction of a μm). Scale of the image: 890 μm × 700 μm. (**c**) D_3 domains at 30°C, $A_m = 20\,\text{Å}^2$. Here some domains are in focus while others are out of focus. Scale of the image: 890 μm × 700 μm. The dark background in figure (b) and (c) is a D_1 domain which appeared grey under the microscope.

To identify the phases in the domains, the monolayer was studied under a polarising microscope in transmission. In this study, the domains were visible only for A_m less than $20\,\text{Å}^2$. Below 28°C, we saw large transparent D_2 domains. At temperatures above 28°C, these transformed into D_3 domains with schlieren textures [12] typical of nematic phase (figure 4a). Interestingly, we also observed in some domains a boojum like texture [13] which corresponds to a point singularity on the domain surface. Some of the boojums were stable (figure 4b) while others changed over to schlieren textures. Above 36°C, the textures in D_3 domains disappeared. These D_3 domains cast shadows which implied their convex lens shape. On cooling, the schlieren textures reappeared in these domains around 36°C. On further cooling, below 28°C, the D_3 domains changed to D_2 in which the textures disappeared except for a few defects at the periphery of the domains.

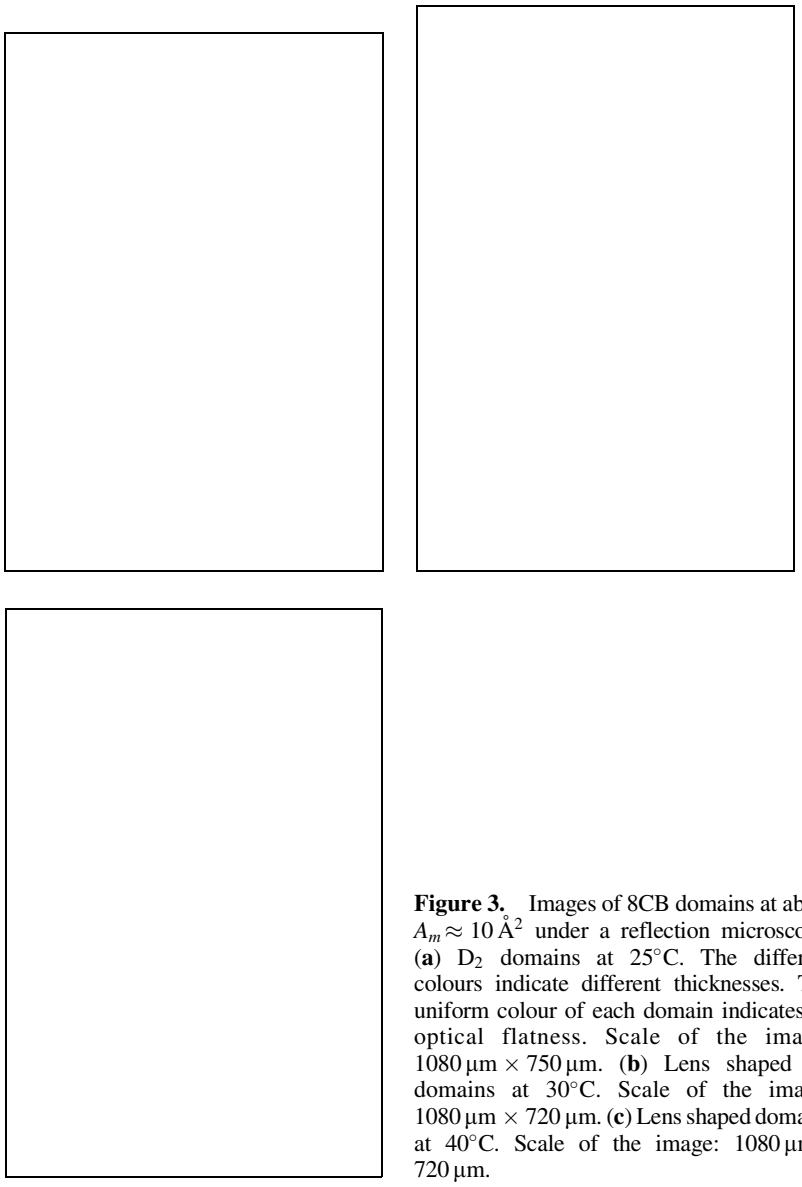

Figure 3. Images of 8CB domains at about $A_m \approx 10\,\text{Å}^2$ under a reflection microscope. (**a**) D_2 domains at 25°C. The different colours indicate different thicknesses. The uniform colour of each domain indicates its optical flatness. Scale of the image: 1080 μm × 750 μm. (**b**) Lens shaped D_3 domains at 30°C. Scale of the image: 1080 μm × 720 μm. (**c**) Lens shaped domains at 40°C. Scale of the image: 1080 μm× 720 μm.

In convergent light, between crossed polaroids, the D_2 domains exhibited colours of non-uniform intensity, while the D_3 domains above 36°C were colourless. This indicated that the D_2 domains were birefringent, while above 36°C the D_3 domains were isotropic. These observations and the optical flatness as seen in reflection, suggest that the D_2 domains were in the smectic A phase.

From these different observations, we find that the 3D domains found for A_m less than $20\,\text{Å}^2$ exhibit different phases depending on temperature. Below 28°C, these domains are

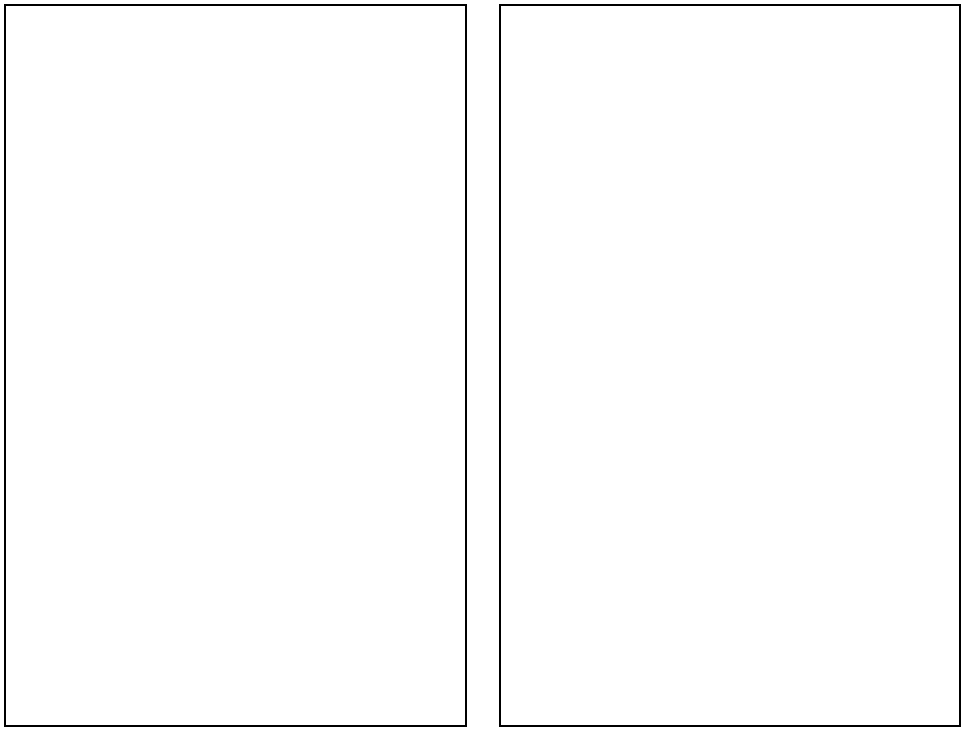

Figure 4. Images of 8CB domains at 30°C around $A_m \approx 10\,\text{Å}^2$ under a polarising microscope (**a**) D_3 domain exhibiting schlieren texture. Scale of the image: $380\,\mu\text{m} \times 270\,\mu\text{m}$. (**b**) Two boojum defects. Scale of the image: $380\,\mu\text{m} \times 270\,\mu\text{m}$.

flat and have a smectic A order. In the range 28°C to 36°C they become lens shaped with a nematic order and above 36°C the domains possess isotropic order.

These studies show that an 8CB monolayer evolves continuously into a 3D liquid crystalline phase on compression. This transformation from the monolayer to the liquid crystalline phase on compression and the reverse transformation to monolayer on expansion indicate that the molecular organisation can be continuously tuned by the surface molecular density. The results may be interpreted to indicate that at high A_m, the intermolecular forces that stabilise the monolayer dominate resulting in adhesion of molecules to the subphase. On the other hand at low A_m, the intermolecular forces that result in liquid crystals dominate leading to a 3D cohesion of molecules.

3. Induced liquid condensed phase and demixing of liquid expanded phase

In the previous section, we saw that in a system like 8CB, a monolayer in the LE phase goes directly to multilayer structures. There are also some cases in which a monolayer in the LE phase goes over to a collapsed state. This happens, for example, in a monolayer of stearic acid (SA) [1]. We discuss the phase diagram of a monolayer of a mixed system of two components *viz.* 8CB and SA. Two interesting features of the phase diagram are an

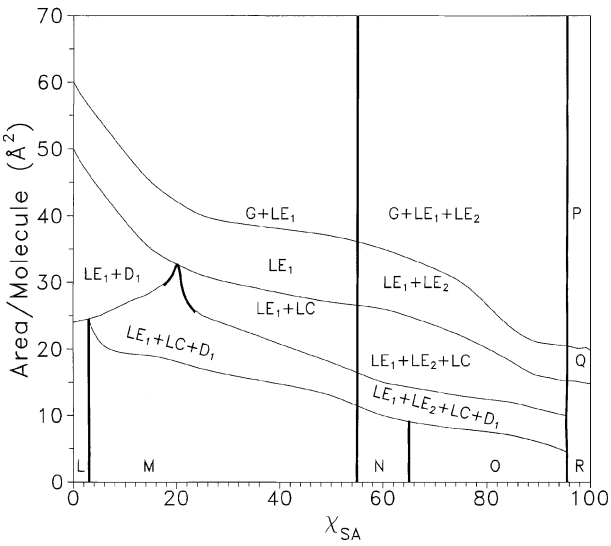

Figure 5. Phase diagram at room temperature for the mixed monolayer system. The thin lines indicate the actual phase boundaries. The thick lines indicate approximate boundaries. [Key: $\mathbf{L} = \mathrm{LE_1} + \mathrm{D_1} + \mathrm{D_2}$, $\mathbf{M} = \mathrm{LE_1} + \mathrm{LC} + \mathrm{D_1} + \mathrm{D_2}$, $\mathbf{N} = \mathrm{LE_1} + \mathrm{LE_2} + \mathrm{LC} + \mathrm{D_1} + \mathrm{D_2}$, $\mathbf{O} = \mathrm{LE_1} + \mathrm{LE_2} + \mathrm{LC} + \mathrm{D_1} + \mathrm{D_3}$, $\mathbf{P} = \mathrm{gas} + \mathrm{LE_2}$, $\mathbf{Q} = \mathrm{LE_2}$, $\mathbf{R} =$ collapsed state]. $\chi_{\mathrm{SA}} =$ molar concentration of SA in 8CB expressed as a molar percentage.

induced LC phase and a phase separation of the LE phase into an 8CB rich LE phase ($\mathrm{LE_1}$) and an SA rich LE phase ($\mathrm{LE_2}$) [14].

The phase diagram depicted in figure 5 has been constructed from the surface manometry and epifluorescence microscopic studies. In the mixtures with upto 3% of SA in 8CB, the phase sequence on compression was that of pure 8CB: $\mathrm{G} + \mathrm{LE_1} \rightarrow \mathrm{LE_1} \rightarrow \mathrm{LE_1} + \mathrm{D_1} \rightarrow \mathrm{LE_1} + \mathrm{D_1} + \mathrm{D_2}$. In the mixtures with 3% to 20% of SA in 8CB, on compressing the monolayer in the $\mathrm{LE_1} + \mathrm{D_1}$ co-existence region, an LC phase appeared. This was followed by $\mathrm{D_2}$ domains. Here the phases $\mathrm{LE_1}$, LC, $\mathrm{D_1}$ and $\mathrm{D_2}$ co-existed as shown in figure 6a, b. The $\mathrm{D_2}$ domains were flat with smectic A order, as suggested by reflection and polarising microscopic studies [11].

For 20% to 55% of SA in the mixture, the LC phase appeared before the onset of the $\mathrm{D_1}$ domains. The isotherm for 25% of 8CB in SA is shown in figure 7. Here the plateau at A_m greater than 40 Å^2 (point (a) in figure 7) is the $\mathrm{G} + \mathrm{LE_1}$ two phase region. The region with steeply increasing π (a to b) corresponds to the $\mathrm{LE_1}$ phase. The change of slope at 27 Å^2 (b) indicates the onset of LC phase. The change of slope at $A_m \approx 22$ Å^2 (c) represents the onset of the $\mathrm{D_1}$ domains.

At SA concentrations between 55% and 95%, another LE phase ($\mathrm{LE_2}$) separated from the $\mathrm{LE_1}$ phase. The $\mathrm{LE_2}$ phase was not as bright as the $\mathrm{LE_1}$ phase but was brighter than the G phase. In figure 8a we show the co-existence of G, $\mathrm{LE_1}$ and $\mathrm{LE_2}$ phases. The $\mathrm{LE_1}$ and $\mathrm{LE_2}$ phases also co-existed with the LC phase at low A_m (figure 8b). Beyond this concentration, the behaviour was like that of pure SA. The $\mathrm{D_1}$ domains appeared first in the $\mathrm{LE_1}$ phase and were followed by the $\mathrm{D_2}$ or $\mathrm{D_3}$ domains. On the other hand, the $\mathrm{LE_2}$

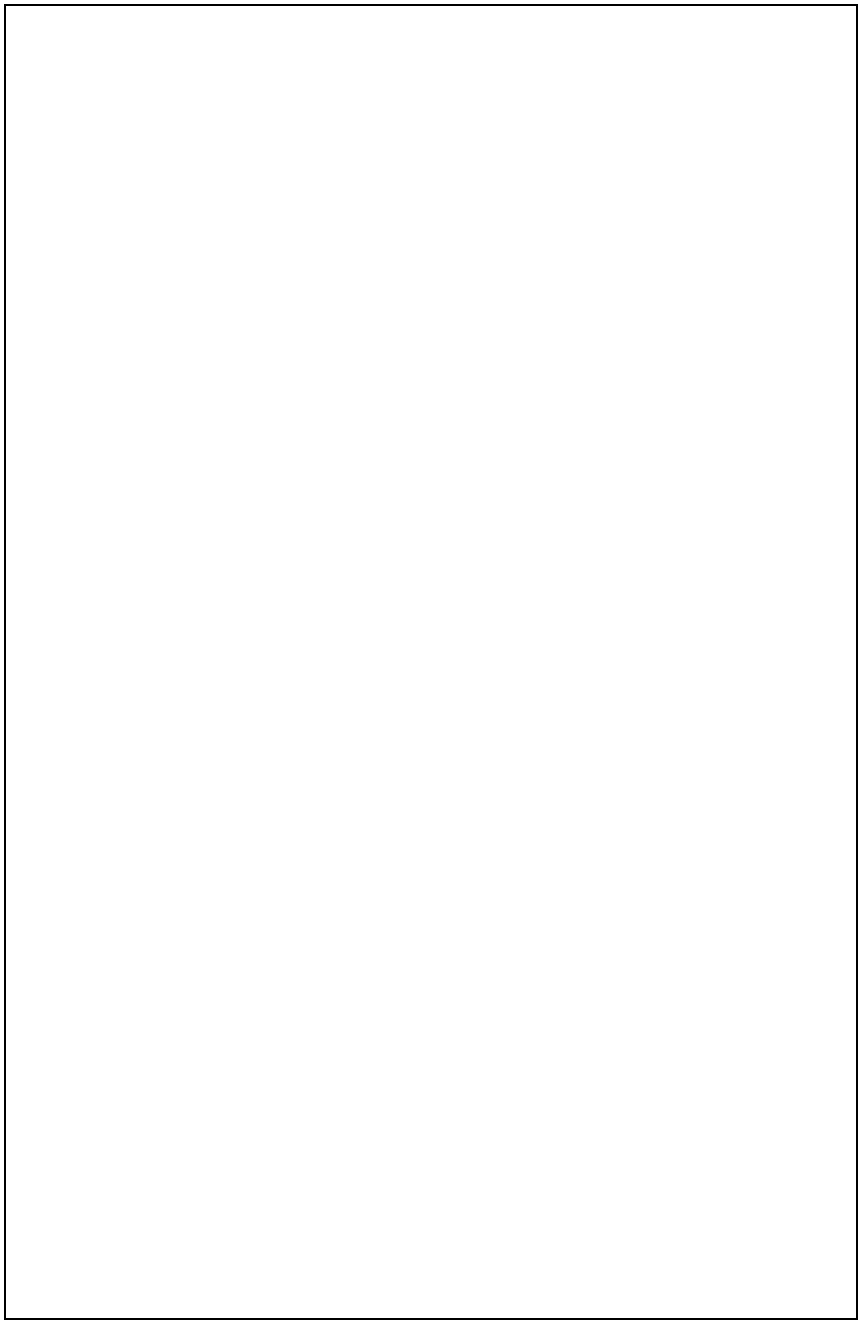

Figure 6. Fluorescence images of a mixed monolayer of 15% SA in 8CB at $A_m \approx 10\,\text{Å}^2$. (**a**) Coexistence of LC (black), LE_1 (grey), D_1 (light grey domain close to the top right corner) and D_2 (bright) domains. Scale of the image: $600\,\mu\text{m} \times 870\,\mu\text{m}$. (**b**) A similar image. The contrast between LE_1 and D_1 domains is not apparent in this figure. Some of the D_2 domains can be seen to be entering into the LC domains. Scale of the Image: $600\,\mu\text{m} \times 600\,\mu\text{m}$.

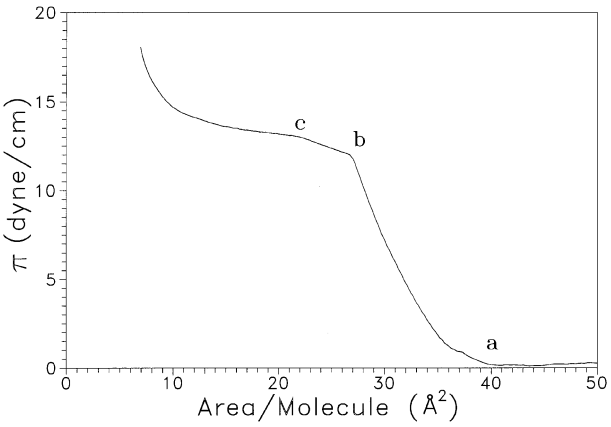

Figure 7. The $\pi - A_m$ isotherm for 25% SA in 8CB at room temperature. The plateau at A_m greater than 40 Å^2 (a) is the G + LE_1 two phase region. The region with steeply increasing π corresponds to pure LE_1 phase. The change of slope at 27 Å^2 (b) indicates the onset of LC phase. The change of slope indicated by (c) is the onset of the D_1 domains. This change of slope was most prominent at this molar concentration. The D_2 domains appeared at $A_m \approx 16$ Å^2.

phase transformed to the D_3 domains directly and rarely transformed to the D_1 domains. The D_3 domains in the LE_2 phase moved much faster than those in the LE_1 phase, indicating that the LE_2 phase is comparatively more fluid than the LE_1 phase.

An interesting feature of the phase diagram is the induction of an LC phase which does not occur in the monolayer of either component. It occurs in mixtures with molar concentrations of 3% to 95% SA in 8CB. Under the fluorescence microscope, this induced phase appeared dark due to expulsion of the dye. This implies that it is a dense phase. Also the monolayer was less mobile. Hence it is identified as the LC phase. This could be L_{2h}, L_{2d} or the fluid lamellar phase. Only x-ray [3] or miscibility [4] studies can reveal the exact phase. Dupin *et al* [15] attribute the absence of two liquid phases in SA to its long chain length. We suggest that the smaller chain length of 8CB molecules brings the effective chain length of the mixture to an appropriate range. Also, Schmid and Schick [10] have pointed out that two liquid phases can be formed due to stiff chains. Hence, the formation of LC phase is further aided by an increase in the chain stiffness, due to the biphenyl group of 8CB. Therefore the mixed monolayer may be considered to be effectively like the monolayer of a fatty acid with shorter and stiffer chains. Another feature of the phase diagram is that for SA molar concentration upto 20%, the D_1 domains appeared first and the LC phase appeared later. On the other hand, at higher SA concentrations, the LC phase preceded the D_1 domains. This behaviour is obviously a result of the subtle nature of the hydrophobic chain – subphase and polar headgroup – subphase interactions involved in the formation of LC and D_1 phases.

An important feature of the phase diagram is the phase separation of the LE phase into LE_1 and LE_2 in the mixed monolayer. Both phases were highly mobile and the dye dissolved in both of them easily. Further, in view of their appearance before LC and after G phases, they can be identified as two LE phases. The LE_1 phase is similar to the L_1 phase.

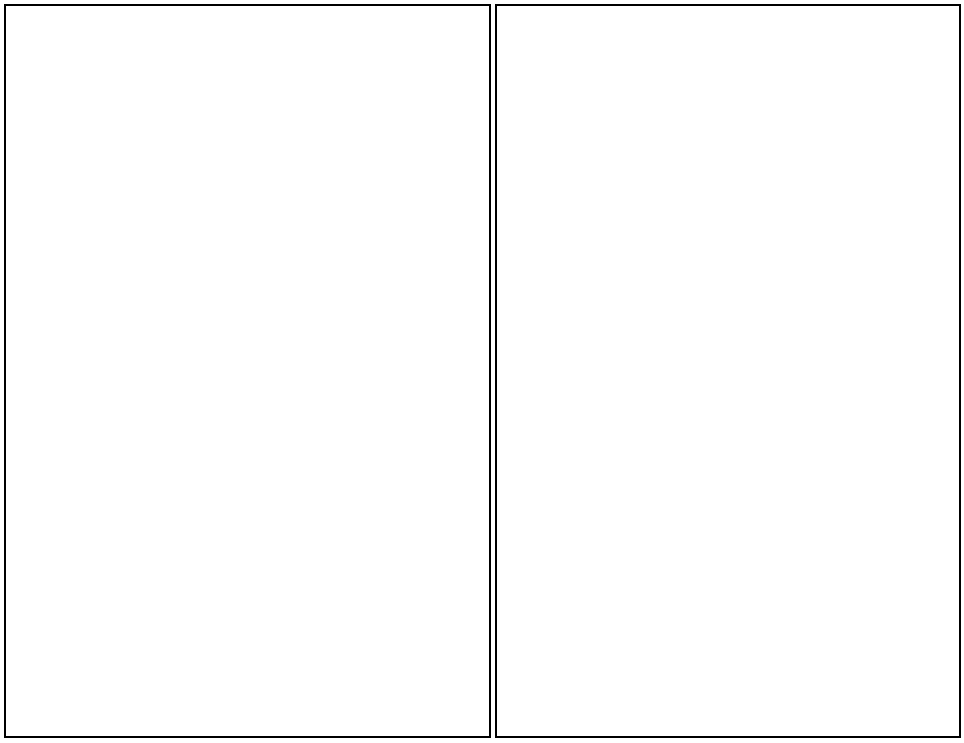

Figure 8. (**a**) Fluorescence images of the mixed monolayer for molar concentration of 75% SA in 8CB. (**a**) Co-existence of G (black domains), LE_2 (grey domains) and LE_1 (bright background) phases. The image is taken at $A_m \approx 50\,\text{A}^2$. Scale of the image: $900\,\mu\text{m} \times 600\,\mu\text{m}$. (**b**) Co-existence of LC (black domains), LE_2 (grey domains) and LE_1 (bright background) phases. The image is taken at $A_m \approx 15\,\text{Å}^2$. Scale of the image: $900\,\mu\text{m} \times 600\,\mu\text{m}$.

The LE_2 phase is more mobile than the LE_1 phase and is likely to be a modified form of the L_1 phase. However, the two phases are distinct as indicated by their clear phase separation. Again a detailed structural identification of the phases is required. Also, transferring the monolayer onto a solid substrate and studying it by atomic force microscopy and x-ray diffraction can yield valuable information. The phase separation and the relative areas occupied by the LE_1 and LE_2 phases at any concentration were independent of the particular dye used. The phase separation started only on increasing SA beyond 55%. At still higher concentrations, the LE_2 phase increased in area at the expense of the LE_1 phase. Further, the multilayer domains, which are characteristic of pure 8CB, always appeared first in the LE_1 phase. In addition, the LE_1 phase had a lower fluidity compared to the LE_2 phase. This points to a higher proportion of 8CB in LE_1 phase, as the larger head-group of 8CB impedes movement. These results taken together indicate that the LE_1 phase is 8CB rich while LE_2 is SA rich.

The co-existence of three stable monolayer phases, such as G, LE_1 and LE_2 (figure 8a) and LE_1, LE_2 and LC (figure 8b) can be accounted for by the Crisp's phase rule [17] for 2D systems. In this mixed monolayer system, the number of degrees of freedom at any

given temperature and pressure is given by

$$F = 3 - q, \tag{2}$$

where q is the number of monolayer phases. Hence, at any fixed temperature, a two component monolayer system can have a maximum of three stable phases. The D_1, D_2 and D_3 domains are 3D structures and hence are not under the perview of this phase rule.

Figure 6b shows that, in the co-existence region, some D_2 domains enter into the LC areas of the monolayer. This may be due to the expulsion of some 8CB molecules which form a D_2 domain over the monolayer. According to Enderle *et al* [18], all the 8CB molecules are squeezed out of the monolayer and they settle above the SA monolayer. But if there is such a total expulsion of 8CB molecules, the A_m value at the peak surface pressure should decrease with higher concentration of 8CB. The experiments do not indicate such a trend. Also, the π value at the onset of collapse for the mixed monolayer was less than that for a pure SA monolayer [18]. Therefore, a partial squeezing out of 8CB molecules is more likely, as seen in 8CB – pentadecanoic acid system [19].

The partial expulsion of 8CB molecules from the monolayer can be attributed to the weak anchoring of 8CB molecules to water. The induction of the LC phase can be accounted for by the reduction of the effective chain length and stiffening of the molecules. But an understanding of the phase separation of the 8CB rich LE_1 phase and the SA rich LE_2 phase calls for an extensive study.

4. Critical points in Langmuir monolayers

The nature of phase transitions in Langmuir monolayers have been a subject of detailed study for a long time. Till recently, the G–LE and LE–LC phase transitions were probed mainly by surface manometry. The G–LE transition was accepted to be first order as a result of a plateau of infinite compressibility in the $\pi - A_m$ isotherms. On the other hand, the nature of the LE–LC transition was somewhat controversial due to the finite though very large compressibility. With the development of new techniques like epifluorescence microscopy it has been established that the LE–LC transition is first order. Associated with both the G–LE and LE–LC transitions, there are critical temperatures above which the phase transition disappears very much like in the classical liquid gas phase transition above the critical temperature (T_c).

There have been several attempts [20–23] to determine T_c corresponding to the G–LE transition, particularly for pentadecanoic acid (PDA). Unfortunately, there are many conflicting results. The earlier values of T_c as reported by Kim and Cannel [20] and Hawkins and Benedek [21] are respectively 26°C and 27°C. On the other hand, the values obtained later by Pallas and Pethica [22] and Rondelez *et al* [23] are in the range of 50°C to 60°C. Rondelez *et al* have estimated T_c associated with LE–LC transition of PDA to be greater than 50°C. In the case of myristic acid (MYA), T_c has been determined to a greater reliability. Suresh *et al* [24] employing surface manometry and epifluorescence microscopy have estimated T_c for MYA to be 31°C. This value is in direct confirmation with the earlier observations of Adam and Jessop [25]. These authors report that the width of the LE–LC plateau region in the isotherm decreases steadily as temperature increases from 7°C to 26°C. Also, there is no plateau at 34.4°C, which is

consistent with the value of 31°C for T_c. In the vicinity of such T_c, one can expect some interesting features. For example, the line tension between the LE and LC phases in the two-phase co-existence region should decrease as the temperature approaches T_c. As a consequence, LC domains in the LE phase exhibit some interesting patterns. We discuss pattern formation of such domains in MYA during the LE–LC phase transition near the critical temperature.

5. Pattern formation in the two-phase region below critical temperature

In the MYA monolayer system, during the LE–LC phase transition, the shape of the LC domains strongly depends on the experimental conditions, especially the temperature relative to T_c. If the monolayer is compressed at constant temperature well below T_c, almost perfect circular disks are found as soon as the two-phase region is entered. Upon further compression, these LC domains grow in size but their number stays fixed, which is typical for a nucleation and growth process. If one repeats the compression at a temperature much closer to T_c, one finds that highly branched structures grow in regions of low nucleation. Stopping the compression immediately inhibits further growth and the branched structures are found to slowly evolve towards circular disks over a few minutes. There is obviously a competition between the growth rate of the instability and the relaxation rate governed by the line tension and viscous forces. Identical structures can also be obtained at fixed molecular density, simply by lowering the temperature from the one phase LE region into the two phase LE–LC region. If the cooling rate is sufficiently rapid, one can find finger-like structures in the vicinity of T_c. These structures evolve into compact morphologies as the temperature is lowered further. The LC domains near T_c grow by splitting their tips. The largest clusters found in these experiments have a diameter of 300 μm. Typically one notices up to three successive splittings, each finger having a constant width of the order of 10 to 20 μm.

In nearly pure systems containing a small amount of impurity and undergoing a phase separation between a solid and a liquid phase, it is generally thought that the growth of dendritic structures is due to constitutional supercooling [26]. For instance, the diffusion of fluorescent molecules away from the interface has been invoked [27] to explain the growth of self-similar patterns in monolayers of phospholipids containing a fluorescent dye. The observation of a large concentration gradient of dye normal to the solid–liquid boundary is in strong support of this explanation. However, several of the observations in MYA doped with NBD–HDA point towards a different mechanism. For example, unstable growth does not seem to depend on the dye concentration. Also, since MYA and NBD–HDA molecules have very similar chemical structures, the segregation effects induced by the presence of NBD–HDA molecules should be minimum. It may be pointed out that in the case of Langmuir monolayers impurity diffusion is not a necessary condition for unstable growth. For example, Mullins and Sekerka [28] have shown that some kind of a diffusing mechanism can lead to unstable growth. In the usual 3D systems studied in metallurgy, this diffusion can only be that of heat or solute impurities. In a 2D monolayer on a fluid substrate, there is another possibility. The motion of the surfactant molecules is strongly coupled to the substrate. One can thus consider that the diffusive mechanism is that of the pure species itself undergoing Brownian diffusion within the monolayer.

In nearly pure substances, the solidification process is governed either by the diffusion of latent heat generated during the phase transition or by the effect of mass transport under concentration gradients [26]. In this context, experiments on 2D monolayers spread on a liquid substrate are especially valuable because they provide a rather unique way of suppressing the thermally controlled instabilility, since the heat can diffuse away from the monolayer vertically into a large thermal bath [1]. Thus the experiment on MYA provides evidence for the unstable growth of LC domains due to mass concentration gradients.

6. Conclusions

Phase transitions in Langmuir monolayers, initially studied by surface manometry, revealed 2D phases such as the gaseous phase, the LE phase, the LC phase and the solid phase. With the advent of new techniques like epifluorescence microscopy, Brewster angle microscopy, x-ray diffraction, miscibility studies, second harmonic generation, surface potential measurement and so on, now we know as many as 17 different 2D phases. Some of the phase transitions are associated with critical points. We have discussed the behaviour near critical points, in particular the critical points associated with the G–LE and LE–LC two phase regions. We have also described the pattern formation in the vicinity of the LE–LC critical point in the case of myristic acid monolayer. In some monolayers like that of 8CB, there are transitions from 2D phases to 3D structures. The characterization of these 3D structures have shown the existence of liquid crystalline order. A study of a mixed monolayer system has indicated induced phases and a hitherto unobserved phase separation of the LE phase. All these examples illustrate a variety of interesting results associated with the phase transitions in Langmuir monolayers and calls for a lot more theoretical and experimental investigations.

References

[1] G L Gaines Jr., *Insoluble Monolayers at Liquid Gas Interface* (Interscience, New York, 1966)
[2] X Qiu, J Ruiz-Garcia, K J Stine, C M Knobler and J V Selinger, *Phys. Rev. Lett.* **67**, 703 (1991)
[3] A M Bibo and I R Peterson, *Adv. Mater.* **2**, 309 (1990)
[4] A M Bibo, C M Knobler and I R Peterson, *J. Phys. Chem.* **95**, 5591 (1991)
[5] M C Shih, T M Bohanon, J M Mikrut, P Zschack and P Dutta, *Phys. Rev.* **A45**, 5734 (1992)
[6] H D Dorfler, W Kerscher and H Sackmann, *Z. Phys. Chem.* **251**, 314 (1972)
[7] K A Suresh, A Blumstein and F Rondelez, *J. Phys.* **46**, 453 (1985)
[8] J Xue, C S Jung and M W Kim, *Phys. Rev. Lett.* **69**, 474 (1992)
[9] M N G de Mul and J A Mann Jr., *Langmuir* **10**, 2311 (1994)
[10] P Schmitz and H Gruler, *Europhys. Lett.* **29**, 451 (1995)
[11] K A Suresh and A Bhattacharyya, *Langmuir* **13**, 1377 (1997)
[12] S Chandrasekhar, Liquid Crystals, 2nd Edition (Cambridge University Press, 1992)
[13] S Riviere and J Meunier, *Phys. Rev. Lett.* **74**, 2495 (1995)
[14] A Bhattacharyya and K A Suresh, *Europhys. Lett.* **41**, 641 (1998)
[15] J J Dupin, J L Firpo, G Albinet, A G Bois, L Casalla and J F Baret, *J. Chem. Phys.* **70**, 2357 (1979)
[16] F Schmid and M Schick, *J. Chem. Phys.* **102**, 2080 (1995)
[17] D J Crisp, *Surface Chemistry Suppl. Research* (Butterworths, London, 1949) pp 17, 23
[18] Th Enderle, A J Meixner and I Zschokke-Granacher, *J. Chem. Phys.* **101**, 4365 (1994)

[19] M Barmentlo and Q H F Vrehen, *Chem. Phys. Lett.* **209**, 347 (1993)
[20] M W Kim and D S Cannel, *Phys. Rev.* **A13**, 411 (1976)
[21] G A Hawkins and G B Benedek, *Phys. Rev. Lett.* **32**, 524 (1974)
[22] N R Pallas and B A Pethica, *Langmuir* **1**, 509, (1985)
[23] F Rondelez, J F Baret, K A Suresh and C M Knobler, *Proc. 2nd Int. Conf. on Physico-Chemical Hydrodynamics* edited by M Velarde, NATO ASI Series, **174**, 857 (Plenum Press, New York, 1988)
[24] K A Suresh, J Nittmann and F Rondelez, *Europhys. Lett.* **6**, 437 (1988)
[25] N K Adam and G Jessop, *Proc. R. Soc. London* **A112**, 362 (1926)
[26] D P Woodruf, *The Liquid – Solid Interface* (Cambridge University Press, Cambridge, UK, 1973)
[27] A Miller, W Knoll and H Mohwald, *Phys. Rev. Lett.* **56**, 2633 (1986)
[28] W W Mullins and R K Sekerka, *J. Appl. Phys.* **34**, 323 (1963)